

Subharmonic Energy-Gap Structure and a Josephson-Radiation-Enhanced Gap in Dayem Bridges

P. E. Gregers-Hansen, E. Hendricks, M. T. Levinsen, and G. R. Pickett*
Physics Laboratory I, H. C. Ørsted Institute, University of Copenhagen, Denmark

(Received 4 June 1973)

Superconducting thin-film microbridges are found to have subharmonic energy-gap structure in their I - V characteristics at voltages of $2\Delta/Ne$, which on the application of microwaves develop sidebands at $2\Delta/Ne \pm M\hbar\omega/Ne$. The structure is explained on the basis of pair breaking by the harmonics of the Josephson radiation, both directly and via the normal electrons. An enhancement of the energy gap apparently induced by the Josephson radiation is observed in the subharmonic structure.

Superconducting thin-film microbridges (Dayem bridges), when sufficiently small or studied close to the transition temperature, show a behavior which can be described by a two-fluid model where the Cooper pairs behave according to the Josephson equations and the normal electrons are governed by the normal resistance.¹ To study departures from this simple behavior we have measured the dynamical resistance dV/dI as a function of voltage and found subharmonic energy-gap structure and their rf-induced sidebands in the I - V characteristics of our bridges. Both the subharmonic structure^{2,3} and the induced sidebands⁴⁻⁶ have previously been observed in tunnel junctions and point contacts. Further, the power dependence of the sidebands was found to be proportional to the squares of Bessel functions,^{5,6} consistent with our data.

Dynamic-resistance curves for one of our bridges at a variety of temperatures are shown in Fig. 1. The Dayem bridges were fabricated by a technique reported earlier,¹ which generally allow us to keep the length and the width of the bridge below $0.5 \mu\text{m}$ for a film thickness of $0.1 \mu\text{m}$. Such small dimensions were in fact necessary and sufficient to observe a regular subharmonic structure. On cooling the thin-film microbridges through the transition temperature, a large number of both sharp and diffuse features begin to appear in the dV/dI curves. At lower temperatures the characteristic structure stabilizes with a large, rather ill-defined peak at the higher voltages, below which there is a much better defined subharmonic structure which falls into a broad series of peaks alternating with a narrow series. When the regular structure has stabilized we can identify the sharp peak (which on the lower trace of Fig. 1 is at a voltage just above $100 \mu\text{V}$) as the gap voltage Δ/e . The whole series of peaks can be associated with subharmonics of

the gap $2\Delta/Ne$, where the narrow series is associated with the even values of N and the broad series with odd values of N . The positions of the peaks do not correspond exactly with the voltages $2\Delta/Ne$, which is of considerable importance as we shall see.

We found that the subharmonic structure was very sensitive to microwaves. A series of dV/dI curves for increasing power at 9.0 GHz is

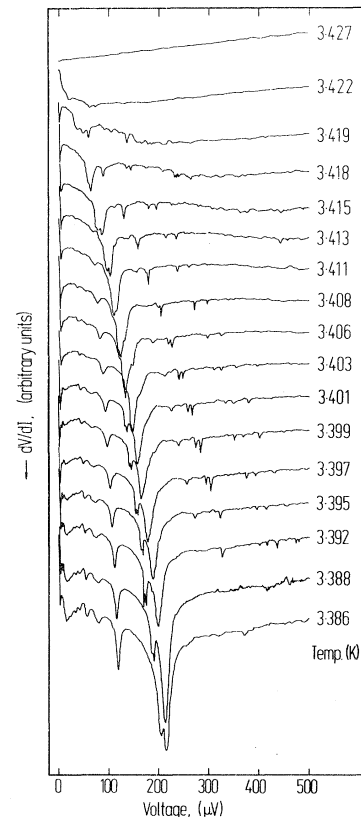


FIG. 1. Dynamic resistance dV/dI versus voltage for an indium Dayem bridge. Recorder traces are shown for successive temperatures below the transition.

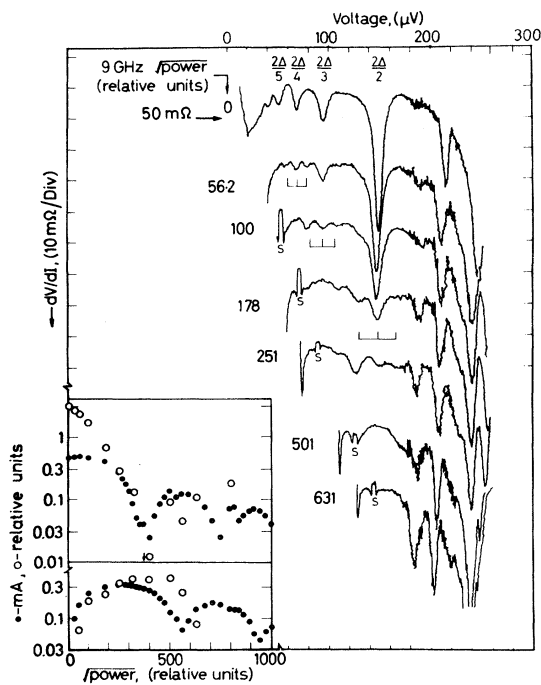


FIG. 2. Dynamic resistance dV/dI versus voltage for various values of microwave power. Induced steps labeled by an S; sideband structure indicated. The height of the peak at $2\Delta/2e$ (top inset, open circles) and its first sideband at $2\Delta/2e \pm \hbar\omega/2e$ (bottom inset, open circles) are shown as a function of the relative microwave field. Here we have also plotted the supercurrent (top inset, solid circles) and the height of the first microwave-induced step (bottom inset, solid circles) versus the same microwave-field at the same temperature $T = 3.365$ K. This In bridge had a maximum supercurrent $2I_0 = 940 \mu\text{A}$ and a maximum height of the first step of $430 \mu\text{A}$ at this temperature. The parameter $\hbar\omega/2eRI_0$ is estimated to be 0.6. From the theoretical expression for the supercurrent (Ref. 1) we derive $\Delta = 0.08$ mV, in fair agreement with the gap structure.

shown in Fig. 2. The resistance level and the supercurrent (see inset) is representative for the bridges studied. The bridges were placed at the end of an X-band waveguide so that we were not troubled by the self-resonance steps induced in a cavity. As the power is increased, the higher subharmonics are rapidly washed out. When this happens to $2\Delta/4e$, we can just begin to see a very diffuse sideband structure before the whole structure is overwhelmed by the steps. Sidebands at $2\Delta/3e \pm \hbar\omega/3e$ then appear on the $2\Delta/3e$ peak, and by the time sidebands appear at $2\Delta/2e \pm \hbar\omega/2e$ we can follow the rise of the sidebands and the reduction of the center peak to zero before the pattern is obliterated by the steps. The large $2\Delta/e$ peak is influenced by the microwaves

but not in any regular way, and we observe no clear progressive sidebands. In the upper inset of Fig. 2 the center peak at $V = 2\Delta/2e$ is plotted as a function of relative microwave field. In the same inset we have also plotted the height of the supercurrent for the same sample at the same temperature. The behavior is similar and both plots are not far from having a variation with the applied microwave power which is like zero-order Bessel functions $J_0(2\alpha I_{rf})$, where I_{rf} is the current set up by the microwave field and α is a constant. Similarly, the sidebands at $2\Delta/2e \pm \hbar\omega/2e$ resemble the dependence of the first step as seen in the lower inset. The higher-order structure at $2\Delta/3e$, $2\Delta/4e$, etc. has a somewhat faster variation with microwave amplitude, not incompatible with Bessel functions of argument $3\alpha I_{rf}$, $4\alpha I_{rf}$, etc.

In both tunnel junctions and point contacts we have observed structures with subharmonic series^{2,3} and induced sideband structure.⁴⁻⁶ To explain these phenomena various successful theories have been put forward.⁷ However, since we find this structure reproducibly occurring in all small bridges tested (both Sn and In), in contrast to tunnel junctions and point contacts, we feel that the suggestion of Rowell and Feldmann² that the majority of such structure is due to metallic shorts is very likely correct.

A peak in the dV/dI curve indicates that the supercurrent is reduced as we increase the voltage through the peak. Thus we look for a process which resonantly suppresses the superconductivity in the bridge. The most obvious candidate for this is pair breaking at the gap frequency $2\Delta/\hbar$ by the Josephson radiation in the weak link itself. Bridges emit radiation at the Josephson frequency and at a large number of higher harmonics, i.e., at frequencies of $2NeV/\hbar$. As we increase the voltage, further pair-breaking mechanisms are provided whenever $2NeV$ reaches 2Δ . On application of radiation which mixes with the bridge frequencies, we expect sidebands at $2NeV \pm \hbar\omega = 2\Delta$, or $eV = (2\Delta \pm \hbar\omega)/2N$. This is precisely the behavior we observe for the even series of subharmonics.

In an analog-computer simulation we have observed the Josephson-radiation amplitude of the bridge at fixed frequency (the gap frequency) as a function of voltage bias, and got a structure very similar to the even series of the measured dV/dI curves. An added external oscillation gives us sidebands at $(2\Delta \pm M\hbar\omega)/2Ne$, with amplitude varying as the M th-order Bessel function

$J_M(2NeRI_T/\hbar\omega)$, where R is the bridge resistance. The subharmonic peaks and the induced sideband structure will then presumably vary with the available power, i.e., as J_M^2 . On the other hand the analog supercurrent and induced steps varied as distorted Bessel functions.¹ In the experimental result shown in the inset of Fig. 2 we can distinguish these two types of behavior.

Thus we are rather confident that the even series is due to some form of detection of the Josephson radiation in the bridge by the energy gap, the rather narrow lines being a reflection of the singularity in the quasiparticle density of states and the well-defined Josephson frequency.

The interpretation of the odd series is less straightforward. We have the experimental observations that the lines are usually broader, and their integrated amplitude larger, than those of the even series, but that their sideband structure under external radiation is very similar to that of the even series. As can be seen in Fig. 2 the $2\Delta/3e$ peak gains sidebands at $(2\Delta \pm \hbar\omega)/3e$ and at a power midway between the points at which sidebands appear on the $2\Delta/4e$ and $2\Delta/2e$ peaks, as one would expect for a uniform series rather than two independent ones. The fact that the series is ruled by odd numbers, we feel, must be a consequence of a mechanism involving normal electrons which on crossing the bridge gain only eV in energy rather than the $2eV$ quanta of the Cooper pairs. One possibility is that a normal electron crosses the bridge gaining eV but while in the bridge is subjected to the ac Josephson frequencies and appears at the other side with eV plus an integral number of Josephson quanta $2NeV$. The quasiparticle now has an energy of $eV + 2NeV$, which it can lose by various processes to drop back to the bottom of the quasiparticle spectrum. If one of these processes can result in pair breaking, then we should observe peaks in the dV/dI curve at $eV = 2\Delta/(2N+1)$, which is consistent with the experimental result. If we furthermore have an external source of microwaves, then we expect pair breaking at $2\Delta = eV + 2NeV \pm \hbar\omega$, i.e., sidebands at $eV = (2\Delta \pm \hbar\omega)/(2N+1)$, again as we observe.

An interesting feature of our experiment is that we can regard the subharmonics in the dV/dI curve as a spectrometric analysis of the gap at various values of the Josephson frequency. In other words we can plot the gap as a function of the Josephson frequency, i.e., the voltage $V = \hbar\omega/2e$. Figure 3 shows such a plot for various temperatures. The most noticeable feature is that,

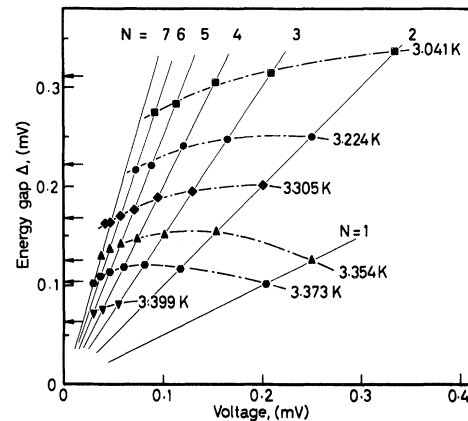


FIG. 3. Energy gap determined from the voltages of the peaks in the dV/dI curve $\Delta = NeV/2$, plotted versus voltage for six different temperatures. The six arrows indicate the indium BCS gap at the same temperatures. Sample same as that shown in Fig. 2.

contrary perhaps to expectation, the gap first increases and then decreases with increasing voltage. This is true for all bridges examined. This might simply mean that the extremity of the subharmonic peak is not the correct place to measure Δ , but any other point of the peak gives a similar behavior. The values of Δ corresponding to the various temperatures calculated from the BCS formula $\Delta = 3.2k_B T_c(1 - T/T_c)^{1/2}$ are shown in the figure by arrows. As can be seen there is enhancement of the energy gap above this value. The voltage at which the maximum enhancement occurs increases with decreasing temperature. This behavior is extremely reminiscent of the increase in the supercurrent caused by externally applied radiation, and Fig. 3 has many features in common with the enhancement of the supercurrent as a function of external frequency given by Dayem and Wiegand.⁸

What we think we are seeing in Fig. 3 is the energy gap in the bridge region increasing as a result of being stimulated by the Josephson radiation. Gap enhancement by microwaves in thin films has been predicted by Eliashberg,⁹ and this effect is in all probability what we observe. Although there is no obvious reason why the predicted phenomena should only occur in constricted films, the general trend, as well as the order of magnitude that the theory suggests is in agreement with the experimental result.

We wish to thank the following persons for discussing their work before publication: L.-E. Hasselberg, B. Kofoed, N. Falsig Pedersen, M. R. Samuelsen, Sidney Shapiro, and O. Hoff-

mann Sørensen. We wish to acknowledge many helpful conversations with J. W. Wilkins during his stay at the H. C. Ørsted Institute. K. Søre Højbjerg is thanked for his help with the analog computations.

*Permanent address: Department of Physics, University of Lancaster, U. K.

¹P. E. Gregers-Hansen and M. T. Levinsen, Phys. Rev. Lett. **27**, 847 (1971).

²J. M. Rowell and W. L. Feldmann, Phys. Rev. **172**, 393 (1968).

³J. E. Zimmermann, in *Proceedings of the Applied Superconductivity Conference, Annapolis, 1972* (Institute of Electrical and Electronics Engineers, New

York, 1972), p. 544.

⁴I. Giaever and H. R. Zeller, Phys. Rev. B **1**, 4278 (1970).

⁵A. Longacre and S. Shapiro, Bull. Amer. Phys. Soc. **16**, 399 (1971).

⁶O. Hoffmann Sørensen, B. Kofoed, N. Falsig Pedersen, and S. Shapiro, in Proceedings of the Danish Solid State Meeting, Munkebjerg, Denmark, 31 May–2 June 1973 (to be published).

⁷L.-E. Hasselberg, M. T. Levinsen, and M. R. Samuelsen, in Proceedings of the Danish Solid State Meeting, Munkebjerg, Denmark, 31 May–2 June 1973 (to be published).

⁸A. H. Dayem and J. J. Wiegand, Phys. Rev. **155**, 419 (1967).

⁹G. M. Eliashberg, JETP Lett. **11**, 114 (1970) [Pis'ma Zh. Eksp. Teor. Fiz. **11**, 186 (1970)].

Test of Tricritical Point Scaling in Dysprosium Aluminum Garnet*

George F. Tuthill,† Fredric Harbus, and H. Eugene Stanley

Physics Department, Massachusetts Institute of Technology, Cambridge, Massachusetts 02139

(Received 4 June 1973)

The scaling hypothesis for a tricritical point has not received any tests from experimental data for magnetic systems. Here, data for dysprosium aluminum garnet are used to test the tricritical scaling hypothesis in the directions \bar{x}_2, \bar{x}_3 lying in the H - T plane. Specifically, M - H - T data near the tricritical point are found to collapse from a family of curves to a single curve (scaling function), supporting the validity of a tricritical scaling hypothesis.

In metamagnetic materials,¹ and in certain model systems,² the "critical line" $H=H_c(T)$ terminates at a certain nonzero temperature T_t , below which there is a line of first-order phase transitions. Griffiths³ has introduced the term "tricritical point" (TCP) to describe the point $[T=T_t, H=H_c(T_t), H_{st}=0]$, where H_{st} denotes the staggered magnetic field.

Dysprosium aluminum garnet (DyAlG) has a tricritical point at $T_t=1.66 \pm 0.01$ K, $H_t=3.25$ kOe, as determined by measurements of Landau *et al.*¹ The TCP scaling hypothesis⁴ implies certain "data collapsing," and, conversely, data collapsing implies TCP scaling. The extent to which experimental data near the TCP collapse onto a single "scaling function" therefore provides a measure of the validity of the TCP scaling hypothesis. In this work we test data collapsing for M - H - T data (for $H_{st}=0$) near the tricritical point in DyAlG.^{5,6}

We formulate the TCP scaling hypothesis in terms of the Gibbs potential $G(H, T)$: Near the TCP, $g \equiv G - G(H_t, T_t) + M_t(H - H_t) + S_t(T - T_t)$ is postulated to be a generalized homogeneous

function, i.e., there exist three numbers ("scaling powers") $\bar{a}_1, \bar{a}_2,$ and \bar{a}_3 such that for all positive λ ,

$$g(\lambda^{\bar{a}_1} \bar{x}_1, \lambda^{\bar{a}_2} \bar{x}_2, \lambda^{\bar{a}_3} \bar{x}_3) = \lambda g(\bar{x}_1, \bar{x}_2, \bar{x}_3). \quad (1)$$

Here S is the entropy and the variables \bar{x}_j are defined at the TCP.⁷

Equation (1) implies that the derivatives and Legendre transforms⁸ of g are also generalized homogeneous functions with scaling powers related to the original scaling powers \bar{a}_j . In particular, we find the TCP exponents $\beta_u, \gamma_u,$ and δ_u (in the Griffiths notation) are expressible in terms of \bar{a}_2, \bar{a}_3 only,

$$\beta_u = \frac{1 - \bar{a}_2}{\bar{a}_3}, \quad -\gamma_u = \frac{1 - 2\bar{a}_2}{\bar{a}_3}, \quad \frac{1}{\delta_u} = \frac{1 - \bar{a}_2}{\bar{a}_2}, \quad (2a)$$

where $\beta_u, \gamma_u,$ and δ_u are defined, respectively, by the relations

$$M^+ - M^- \sim |T_t - T|^{\beta_u}, \quad \chi \sim |T - T_t|^{-\gamma_u}, \\ M - M_t \sim |H - H_t|^{1/\delta_u}. \quad (2b)$$

Eliminating \bar{a}_2, \bar{a}_3 from (2a), we obtain the TCP